

# Blockade of PAR1 Signaling with Cell-Penetrating Peptiducins Inhibits Akt Survival Pathways in Breast Cancer Cells and Suppresses Tumor Survival and Metastasis

Eric Yang,<sup>1,3,4</sup> Adrienne Boire,<sup>1,4</sup> Anika Agarwal,<sup>1,2,3</sup> Nga Nguyen,<sup>1</sup> Katie O'Callaghan,<sup>1</sup> Powen Tu,<sup>5</sup> Athan Kuliopulos,<sup>1,2,3,4</sup> and Lidija Covic<sup>1,2,3,4</sup>

<sup>1</sup>Molecular Oncology Research Institute and <sup>2</sup>Division of Hematology/Oncology, Tufts Medical Center; Departments of <sup>3</sup>Medicine and <sup>4</sup>Biochemistry, Tufts University School of Medicine; <sup>5</sup>Department of Molecular Medicine, Boston University School of Medicine, Boston, Massachusetts

## Abstract

**Protease-activated receptor 1 (PAR1) is a G protein-coupled receptor that is not expressed in normal breast epithelia but is up-regulated in invasive breast carcinomas. In the present study, we found that matrix metalloprotease-1 (MMP-1) robustly activates the PAR1-Akt survival pathway in breast carcinoma cells. This process is blocked by a cell-penetrating lipopeptide "peptiducin," P1pal-7, which is a potent inhibitor of cell viability in breast carcinoma cells expressing PAR1. Both a MMP-1 inhibitor and P1pal-7 significantly promote apoptosis in breast tumor xenografts and inhibit metastasis to the lungs by up to 88%. Dual therapy with P1pal-7 and Taxotere inhibits the growth of MDA-MB-231 xenografts by 95%. Consistently, biochemical analysis of xenograft tumors treated with P1pal-7 or MMP-1 inhibitor showed attenuated Akt activity. Ectopic expression of constitutively active Akt rescues breast cancer cells from the synergistic cytotoxicity of P1pal-7 and Taxotere, suggesting that Akt is a critical component of PAR1-dependent cancer cell viability. Together, these findings indicate that blockade of MMP1-PAR1 signaling may provide a benefit beyond treatment with Taxotere alone in advanced, metastatic breast cancer.** [Cancer Res 2009;69(15):6223–31]

## Introduction

Breast cancer is the most common malignancy in females in the United States and is a leading cause of cancer death second only to lung cancer (1). Metastatic disease has a particularly poor prognosis, and current chemotherapeutic regimens are unlikely to result in complete remission (2, 3). Combining targeted inhibitors of oncogenic proteins with traditional cytotoxic agents has resulted in improved rates of patient response; however, given the heterogeneous nature of cancer and the high rate of reoccurrence (4, 5), there is still a need to identify novel oncogenic targets that can enhance chemotherapeutic vulnerability to resistant disease.

The protease-activated receptor 1 (PAR1) G protein-coupled receptor emerges as a promising oncogenic target because of its involvement in the invasive and metastatic processes of cancers of the breast, ovaries, lung, colon, prostate, and melanoma (6–11).

Recent studies showed that PAR1 promotes tumorigenicity, invasion, and metastasis in breast and ovarian carcinoma xenograft models (12, 13). PAR1 is activated by proteolytic cleavage and release of a tethered ligand by serine proteases, such as thrombin, plasmin, factor Xa, and activated protein C (14, 15).

Recent studies identified matrix metalloprotease-1 (MMP-1) as a novel protease agonist of tumor, platelet, and endothelial PAR1; however, the signaling components have not been characterized (12, 13, 16, 17). Overexpression of MMP-1 is associated with poor prognosis of breast, colorectal, and esophageal cancers (18–20); therefore, understanding the pathophysiologic role of MMP-1 in tumor progression is of great interest. Here, we explore the significance of PAR1 and MMP-1 signaling and its blockade on downstream cell survival pathways in breast cancer cells and xenograft models.

To efficiently block PAR1 signaling, we developed a highly stable, cell-penetrating peptiducin, P1pal-7, that acts as an antagonist of PAR1-G-protein signaling (13, 21). In this study, we show the utility of P1pal-7 as an effective PAR1 antagonist in mouse models of breast cancer. P1pal-7 was cytotoxic only to breast carcinoma cells expressing PAR1 and blocked the PAR1-mediated Akt signal. Dual therapy with P1pal-7 and Taxotere inhibited the growth of MDA-MB-231 xenografts by up to 95% and induced apoptosis through an Akt-dependent mechanism. Blockade of either MMP-1 or PAR1 significantly induced apoptosis in breast xenografts and also inhibited metastasis to the lung. These data implicate MMP1-PAR1-Akt axis as a promising new target for the treatment of breast cancer.

## Materials and Methods

### Reagents

*N*-palmitoylated peptides P1pal-7 and P1pal-19EE and the PAR1 agonist peptide SFLLRN were synthesized as described previously with C-terminal amides (12, 13, 21). Taxotere (docetaxel), 3-(4,5-dimethylthiazol-2-yl)-2,5-diphenyltetrazolium bromide (MTT), propidium iodide, and insulin were purchased from Sigma-Aldrich. RWJ-56110 was a generous gift from Johnson & Johnson. The plasmid pcDNA3-Myr-HA-Akt1 (plasmid #9008) was obtained from Addgene (22). Pro-MMP-1 and FN439 were obtained from Calbiochem. Activation of pro-MMP-1 with APMA was done as described previously (12, 13).

### Cell Culture

MDA-MB-231, MCF7, Bt549, and T47D breast cancer cells were obtained from the National Cancer Institute. The MCF7 cells stably expressing PAR1 (MCF7-PAR1/N55 and N26 clones) were generated in our laboratory as described previously (13). Fibroblast conditioned medium was derived from WI-38 and NIH3T3 cells as described previously (12, 13). MMP-1 was measured using the pro-MMP-1 ELISA kit (R&D Systems) following the manufacturer's protocols.

**Note:** Supplementary data for this article are available at Cancer Research Online (<http://cancerres.aacrjournals.org/>).

**Requests for reprints:** Lidija Covic, Molecular Oncology Research Institute, Division of Hematology/Oncology, Tufts Medical Center, Box 7510, 750 Washington Street, Boston, MA 02111. Phone: 617-636-4665; Fax: 617-636-7855; E-mail: lcovic@tuftsmedicalcenter.org.

©2009 American Association for Cancer Research.  
doi:10.1158/0008-5472.CAN-09-0187

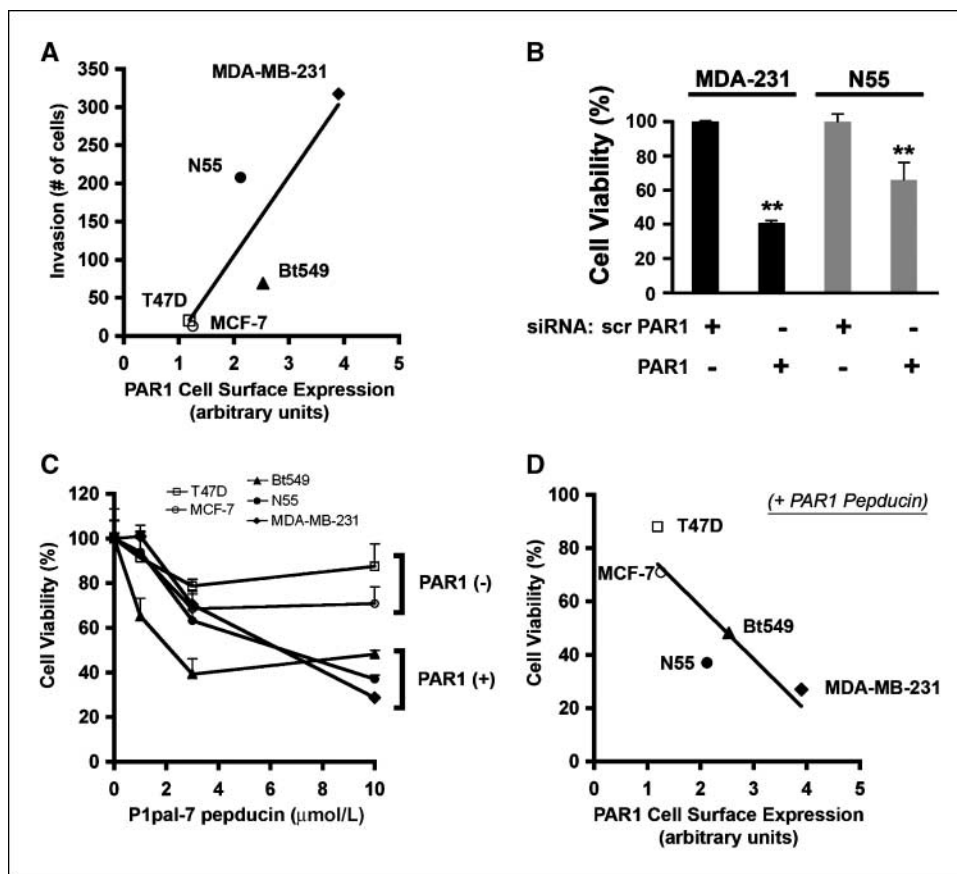


**Figure 1.** PAR1 expression enhances breast cancer cell invasion and survival and confers sensitivity to P1pal-7 pepducin. **A**, MDA-MB-231, MCF7-PAR1/N55, MCF7, T47D, and Bt549 breast cancer cell lines were evaluated for ability to invade through an 8  $\mu$ m pore membrane coated with Matrigel toward NIH-3T3 fibroblast conditioned medium ( $R = 0.76$ ;  $P < 0.05$ ). **B**, MDA-MB-231 and MCF7-PAR1/N55 cells were transfected with siRNA against PAR1 or scrambled sequence PAR1 siRNA (*scr PAR1*). After 72 h, cell viability was evaluated by the MTT assay. **C**, breast carcinoma cells were treated with P1pal-7 pepducin at varying concentrations as indicated for 72 h and cell viability was evaluated by the MTT assay. **D**, cell viability at 10  $\mu$ mol/L P1pal-7 was correlated with relative PAR1 expression ( $R = 0.76$ ;  $P < 0.05$ ). PAR1 expression was analyzed by flow cytometry. Representative data (mean  $\pm$  SD) from multiple experiments. \*\*,  $P < 0.01$ .

### Small Interfering RNA

Small interfering RNA (siRNA) against PAR1 (5'-GGCUACUAUGCCUACUACU-3'; ref. 12), scrambled PAR1 (5'-GCUAAGUUGCACCUCUACU-3'), Akt1 (5'-AAGGAGGUUGCUGCACAAA-3'), Akt2 (5'-AACUUCUCCGUAGCAGAAUGC-3'), Akt3 (5'-AACUGGAGGCCAAGAUACUUC-3'), and firefly luciferase (5'-CGTACGCGGAATACTTCGA-3') were synthesized by Dharmacon.

### MTT Assay

Cells in 96-well plates were subjected to various treatment conditions or vehicle (0.2% DMSO) for 72 h. MTT reagent was added at a concentration of 0.5 mg/mL and allowed to incubate at 37°C for 5 h. The resulting formazan crystals were dissolved with 100% DMSO and absorbance was measured on a SPECTRAmax 340 microplate reader (Molecular Devices).

### Invasion and Wound-Healing Assays

Invasion assays were conducted using Transwell chambers (Corning) with 8  $\mu$ m pore membranes coated with Matrigel as described previously (12, 23). Wound-healing assays were conducted by seeding cells on to glass slides. Confluent monolayers were wounded using a 200  $\mu$ L pipette tip.

### PAR1 Surface Expression

Breast carcinoma cells were labeled with the PAR1 polyclonal SFLLR antibody and a FITC goat anti-rabbit antibody (Zymed) and quantified by fluorescence-activated cell sorting as described previously (13, 14, 23, 24).

### Human Breast Cancer Xenograft in Nude Mice

All experiments were conducted in full compliance with the Institutional Animal Care and Use Committee of Tufts Medical Center. Female NCR *nu/nu* mice (Taconic Farms) each received mammary fat pad injections (cells suspended in 100  $\mu$ L serum-free RPMI with 20  $\mu$ g/mL Matrigel) or tail-vein injections (cells suspended in 200  $\mu$ L PBS). Vehicle (10% DMSO), P1pal-7, and FN439 were administered by s.c. injections (100  $\mu$ L) every other day,

and Taxotere was administered by i.p. injection (100  $\mu$ L) once a week unless otherwise indicated.

**Tumor measurements.** Tumor length ( $L$ ) and width ( $W$ ) were measured with a caliper and volume was calculated by the equation:  $V = (L \times W^2) / 2$ . Images of xenograft tumors were taken using a Xenogen IVIS 200 Biophotonic Imager.

**Histology.** Formalin-fixed tumors were sent to IDEXX Laboratories for terminal deoxynucleotidyl transferase-mediated dUTP nick end labeling (TUNEL) analysis. Formalin-fixed lungs were paraffin embedded, sectioned at three representative depths along the coronal plane, and stained with H&E at the Department of Pathology of Tufts Medical Center. Metastatic tumor nodules were counted throughout the entire lung section at all three depths under a light microscope. Microscopy images were captured with a light microscope and SPOT digital camera (Diagnostic Instruments).

### Statistical Analysis

All quantified xenograft and *in vitro* assay results are presented as mean  $\pm$  SD or mean  $\pm$  SE. Comparisons were made with the Student's  $t$  test. Statistical significance was defined as \*  $P < 0.05$ , \*\*  $P < 0.01$ , or \*\*\*  $P < 0.001$ .

## Results

**P1pal-7 is cytotoxic to invasive breast cancer cells expressing PAR1.** To investigate whether PAR1 expression correlates with invasiveness of breast carcinoma cells, we conducted invasion assays using Matrigel-coated Boyden chambers. Three PAR1-expressing breast carcinoma cells Bt549, MCF7-PAR1/N55, and MDA-MB-231 and two PAR1-null cells T47D and MCF7 were tested for invasion through Matrigel toward fibroblast conditioned medium and correlated with PAR1 cell surface expression (measured by flow cytometry). Total PAR1 protein levels were also confirmed by Western blot (Supplementary Fig. S1A). There was a

positive correlation ( $R = 0.76$ ;  $P < 0.05$ ) between PAR1 surface expression and cellular invasion through Matrigel (Fig. 1A). MCF7-PAR1/N55 is a clonal derivative of MCF7 cells generated by the stable transfection of PAR1 (13, 24). The 20-fold increase in invasive capacity of N55 (compared with MCF7) strongly supports the role of PAR1 in breast carcinoma cell invasion.

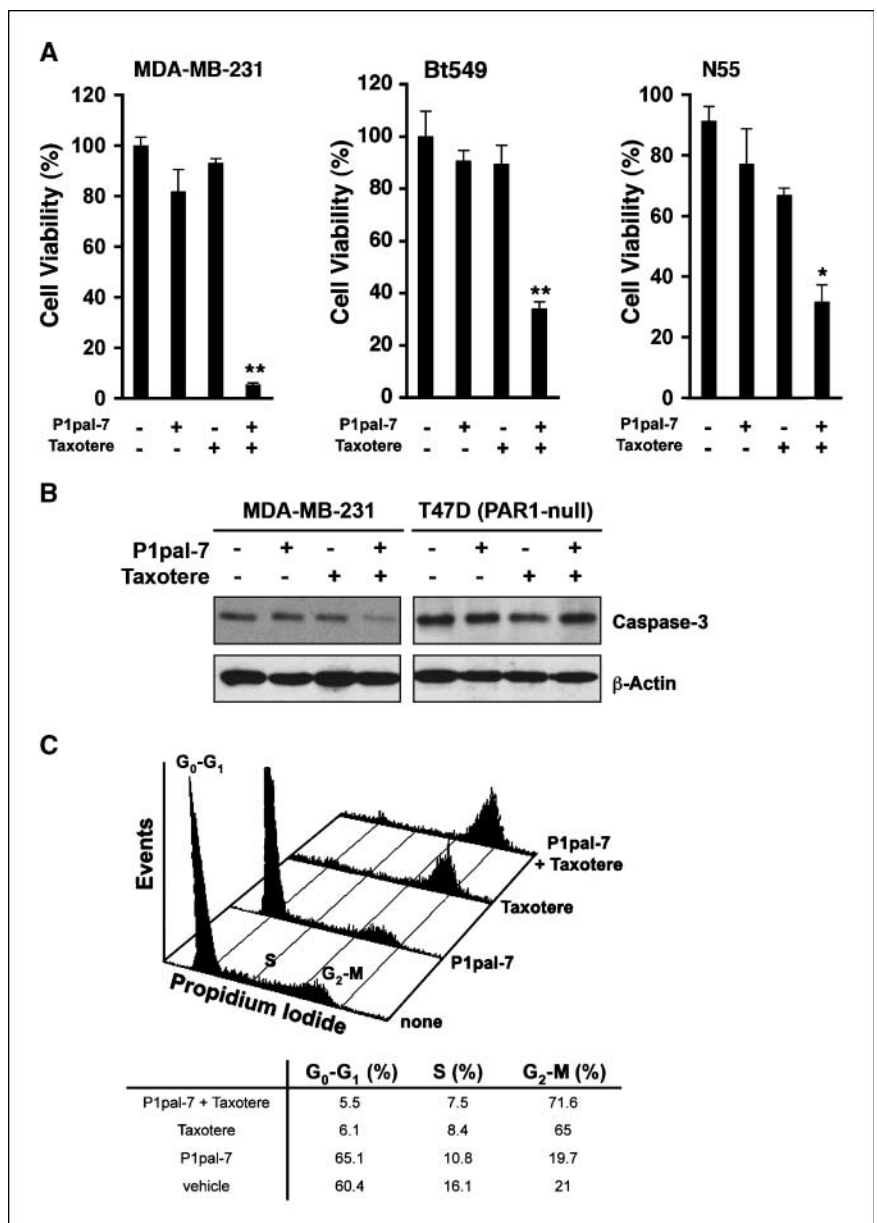
We also followed cell migration and proliferation by wound healing (scratch assay) of PAR1-expressing (N55 and Bt549) and PAR1-null (MCF7 and T47D) cell lines. PAR1-expressing cell lines were able to close the wound within 72 h, whereas PAR1-null MCF7 and T47D cells did not show any significant proliferation or migration into the wounded area (Supplementary Fig. S1B). Again, the difference in migration between the parental PAR1-null MCF7 and PAR1-expressing N55 (MCF7-PAR1) strongly supports the role of PAR1 in cell movement and proliferation.

We then studied cellular proliferation to test for PAR1-mediated survival and proliferative advantages under nutrient-poor conditions. The high PAR1-expressing MDA-MB-231 cells proliferate

36-fold more quickly than the PAR1-null MCF7 cells compared over 7 days (Supplementary Fig. S1C). N55 (medium PAR1 surface expression) and N26 (low PAR1 surface expression) showed a 16- and 5-fold increase in proliferation, respectively, showing a dose response in PAR1-mediated cell growth. We then treated two PAR1-expressing cell lines, MDA-MB-231 and N55, with PAR1 siRNA (13) that decreased cell viability by 75% and 40%, respectively, relative to the scrambled PAR1 control siRNA (Fig. 1B). We achieved almost complete inhibition of PAR1 surface expression with PAR1 siRNA as assessed by fluorescence-activated cell sorting analysis (Supplementary Fig. S1D).

Given that PAR1 siRNA decreased cell viability, we tested whether the PAR1 antagonist pepducin, P1pal-7, would confer cytotoxicity to breast carcinoma cells. A panel of breast cancer cells was treated with varying concentrations of P1pal-7 and cell viability was assessed using either MTT or trypan blue exclusion assays. PAR1-expressing cell lines (MDA-MB-231, Bt549, and N55) were sensitive to P1pal-7, whereas both PAR1-null cell lines, MCF7

**Figure 2.** Dual treatment with P1pal-7 and Taxotere synergistically inhibits cell viability and promotes apoptosis in PAR1-expressing breast carcinoma cells. **A**, MDA-MB-231, Bt549, and MCF7-PAR1/N55 cells were treated with 1  $\mu\text{mol/L}$  P1pal-7, 0.3 nmol/L Taxotere, or both, incubated for 72 h, and evaluated for cell viability by the MTT assay. **B**, MDA-MB-231 and T47D (PAR1-null) cells were treated as indicated above. Lysates were immunoblotted with anti-caspase-3.  $\beta$ -Actin was used as loading control. **C**, MDA-MB-231 cells were treated with 5  $\mu\text{mol/L}$  P1pal-7, 100 nmol/L Taxotere, or both and incubated overnight (18 h). Cells were then stained with propidium iodide and evaluated for cell cycle distribution by flow cytometry. Representative data (mean  $\pm$  SE) from multiple experiments. \*,  $P < 0.05$ ; \*\*,  $P < 0.01$ .



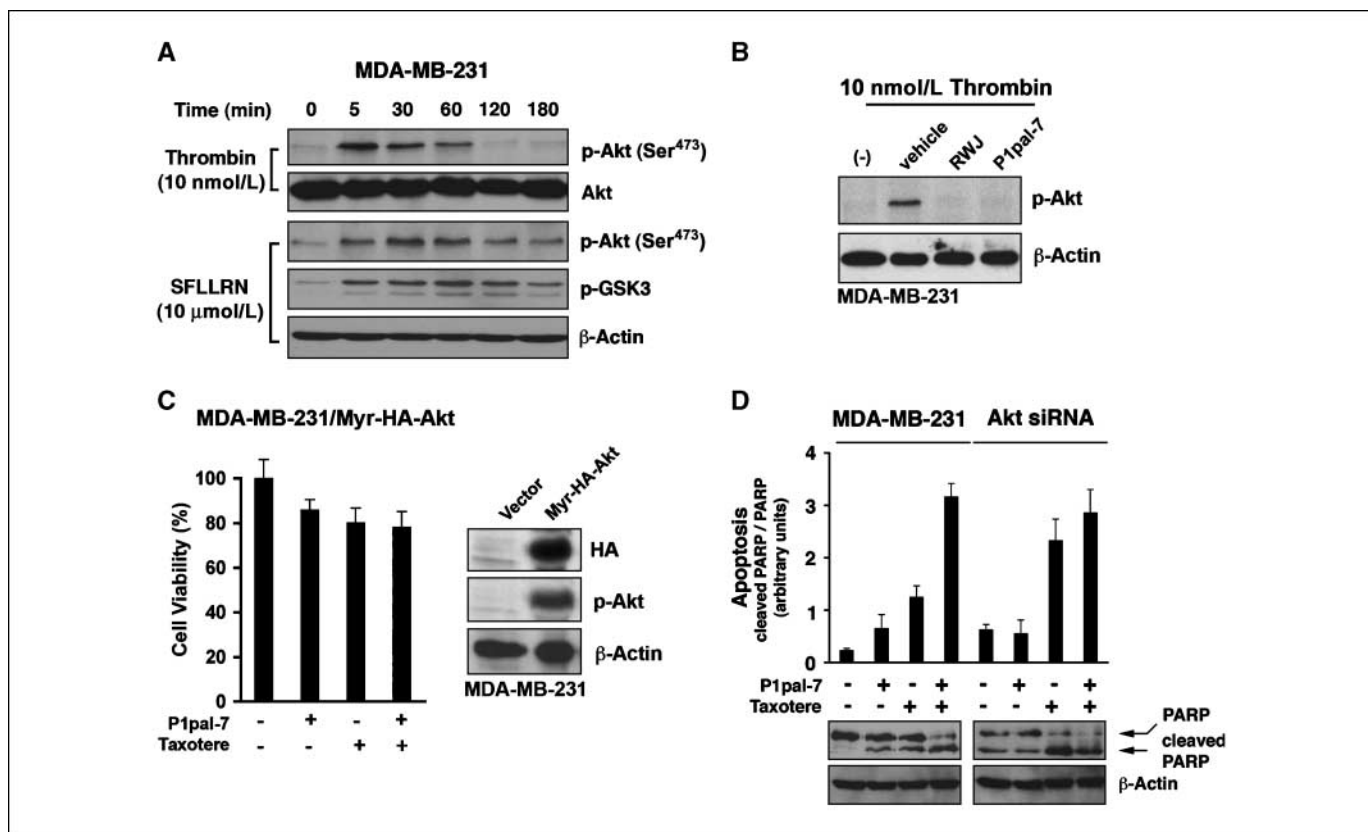


**Figure 3.** PAR1-Akt signaling in breast carcinoma cells. **A**, MDA-MB-231 cells were starved overnight in serum-free medium and stimulated with 10 nmol/L thrombin or 10  $\mu$ mol/L SFLLRN-activating peptide over a period of 3 h. Cell lysates were immunoblotted with anti-phospho-Akt (Ser<sup>473</sup>) or anti-phospho-glycogen synthase kinase 3 (*p*GSK3; Ser<sup>21</sup>/Ser<sup>9</sup>).  $\beta$ -Actin and total Akt were used as loading controls. **B**, MDA-MB-231 cells were pretreated with 3  $\mu$ mol/L P1pal-7 and 5  $\mu$ mol/L RWJ-56110 and subsequently stimulated with 10 nmol/L thrombin. Cell lysates were immunoblotted with anti-phospho-Akt (Ser<sup>473</sup>) at the 5 min time point.  $\beta$ -Actin was used as loading control. **C**, MDA-MB-231 cells were transiently transfected with Myr-HA-Akt or vector control. Cells were treated with 1  $\mu$ mol/L P1pal-7, 0.3 nmol/L Taxotere, or both, incubated for 72 h, and evaluated for cell viability by the MTT assay. Cell lysates were immunoblotted with anti-phospho-Akt (Ser<sup>473</sup>) and anti-HA tag to evaluate transfection efficiency.  $\beta$ -Actin was used as loading control. **D**, MDA-MB-231 and MDA-MB-231 transfected with Akt siRNA were treated with 5  $\mu$ mol/L P1pal-7, 100 nmol/L Taxotere, or both overnight (18 h). Cell lysates were immunoblotted with anti-PARP.  $\beta$ -Actin was used as a loading control. Columns, densitometric measurements of PARP bands normalized to  $\beta$ -actin. Representative data (mean  $\pm$  SD) from multiple experiments.

and T47D, retained high cell viability ( $\geq 70\%$ ) for all P1pal-7 concentrations tested (Fig. 1C; Supplementary Fig. S2A-C). We observed a negative correlation ( $R = 0.76$ ;  $P < 0.05$  and  $R = 0.89$ ;  $P < 0.016$ ) between cell viability and PAR1 expression in the presence of P1pal-7 with both MTT (Fig. 1D) and trypan blue exclusion assay (Supplementary Fig. S2B). Together, these results suggest that PAR1 promotes viability of breast carcinoma cells and renders the PAR1-expressing cells sensitive to the PAR1 pepducin, P1pal-7.

**Synergistic cytotoxicity of pepducin-Taxotere combination therapy activates caspase-mediated apoptosis.** Docetaxel (Taxotere) is considered as the standard-of-care chemotherapeutic agent for the treatment of metastatic breast cancer and other carcinomas. Therefore, we tested whether addition of Taxotere would provide synergistic effects with the PAR1 antagonist P1pal-7 on cell viability using sub-IC<sub>50</sub> amounts of Taxotere and P1pal-7. We varied the concentration of P1pal-7 and found that the IC<sub>50</sub> for cell viability was 1.7  $\mu$ mol/L (Supplementary Fig. S3A), whereas the IC<sub>50</sub> for Taxotere was 1.1 nmol/L (data not shown). Given together, P1pal-7 (1  $\mu$ mol/L) and Taxotere (0.3 nmol/L) decreased cell viability by 95%, 70%, and 70% in MDA-MB-231, Bt549, and N55 cells, respectively (Fig. 2A). Neither P1pal-7 nor Taxotere alone significantly affected cell viability as evaluated by the MTT assay.

The isobologram technique and the Chou and Talalay analysis (25) were employed to quantify the degree of synergy. At various concentrations of P1pal-7 and Taxotere, the isobologram technique indicated strong synergism with a combination index of 0.17 (Supplementary Fig. S3B), which was further confirmed by the Chou and Talalay analysis (Supplementary Fig. S3C). This robust cytotoxic synergy between P1pal-7 and Taxotere may suggest a promising therapeutic potential of combination therapy between PAR1 blockade and the standard-of-care therapy in breast cancer.

We then assessed the involvement of apoptotic pathways to better understand the molecular mechanism underlying the synergistic cytotoxicity between P1pal-7 and Taxotere. Elevated pan-caspase activity was detected in both MDA-MB-231 and N55 cells given combination treatment (Supplementary Fig. S4A and B). Specifically, caspase-3 cleavage and activation correlated closely with decrease in cell viability. Twenty-four hours after treatment initiation, cell viability does not decrease and caspase-3 remains inactive (Supplementary Fig. S4C and D). However, after 72 h of drug treatment, we observed near-complete activation of caspase-3 (Fig. 2B) with a corresponding precipitous decrease in cell viability (Fig. 2A). Caspase-3 activation is not observed in T47D, a PAR1-null breast carcinoma cell line (Fig. 2B). Together, the above results suggest that the P1pal-7/Taxotere combination therapy causes

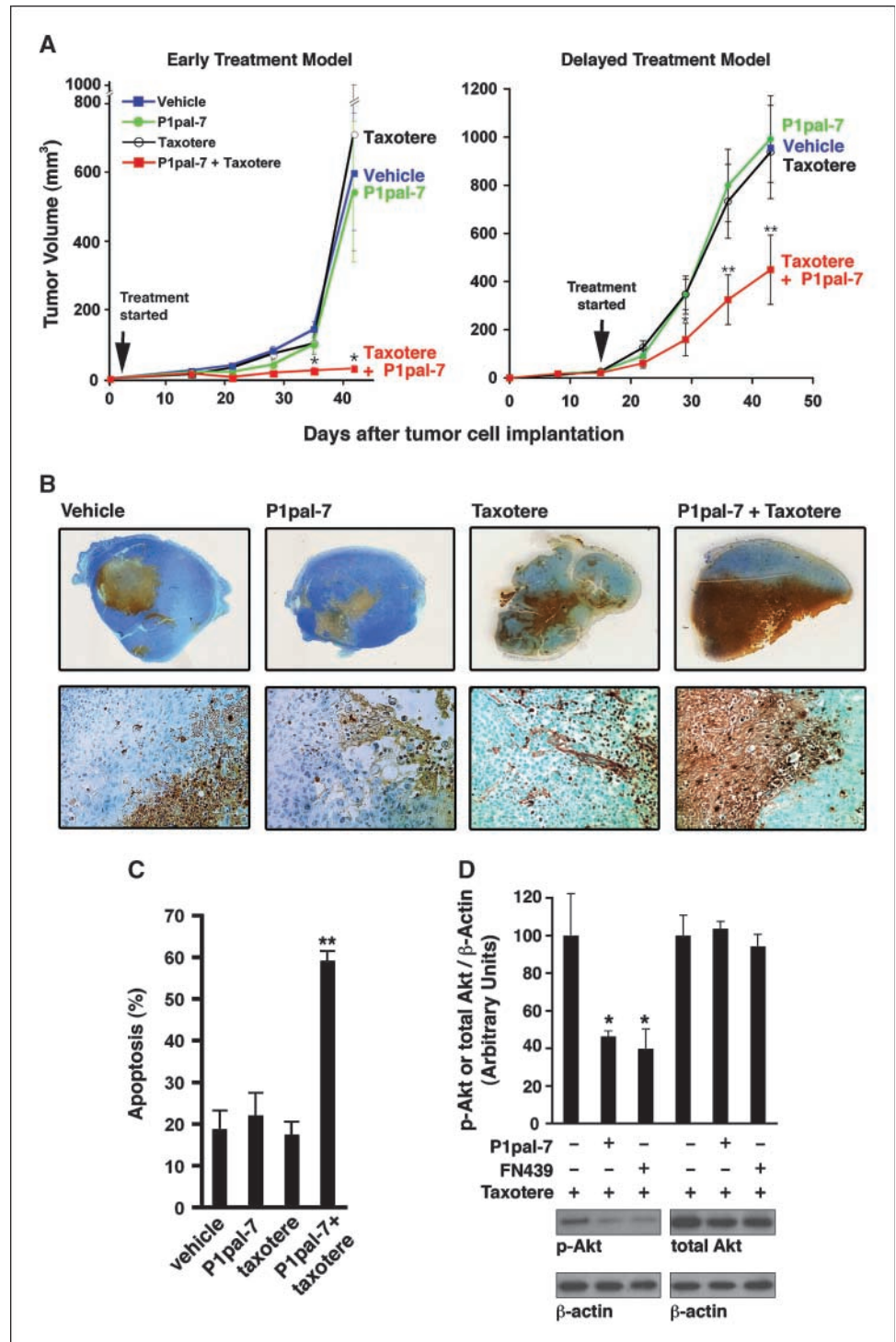
synergistic cytotoxicity by induction of caspase-3-mediated apoptosis pathways in PAR1-expressing breast carcinoma cell lines.

Taxotere by itself confers cytotoxicity by interfering with the dynamics of microtubule assembly and thereby halting the cell cycle at the G<sub>2</sub>-M phase. We confirmed that when MDA-MB-231 cells were treated with Taxotere, the G<sub>2</sub>-M peak increased significantly (65%; Fig. 2C). However, P1pal-7 did not affect cell cycle distribution whether it was administered alone or in combination with Taxotere. These results suggest that Taxotere is

conferring cytotoxicity to MDA-MB-231 through a cell cycle arrest mechanism, whereas P1pal-7 is acting in a pathway independent of cell cycle regulation.

**Activated form of Akt blocks P1pal-7 apoptotic effect in breast carcinoma cells.** Because synergistic inhibition of cell viability and enhanced apoptosis was dependent on PAR1, we examined the effects of PAR1 activation on Akt signaling in breast carcinoma cells. Akt, a serine/threonine kinase, plays a prominent role in cellular growth, metabolism, proliferation, and survival (26)

**Figure 4.** Dual treatment with P1pal-7 peptiducin and Taxotere significantly attenuates growth of mice xenograft breast tumors by promoting apoptosis. **A**, early treatment model: MDA-MB-231 cells ( $4 \times 10^6$ ) were injected into the mammary fat pads of female nude mice. After 2 d, injections with vehicle (10% DMSO), P1pal-7 (10 mg/kg), Taxotere (10 mg/kg), or the combination were initiated ( $n = 5$  mice per group). Delayed treatment model: MDA-MB-231/GFP cells ( $4 \times 10^6$ ) were implanted. Treatment injections as above were initiated 15 d post-implantation ( $n = 10-15$  mice per group). Tumor volumes (mean  $\pm$  SE). **B**, TUNEL analysis of xenograft tumor sections. *Top row*, macroscopic view of tumor sections with TUNEL; *bottom row*, representative fields of xenograft tumor sections (magnification,  $\times 20$ ). **C**, percentage of apoptotic area (mean  $\pm$  SE) of tumor sections as quantified by the ImageJ software. % Apoptosis = (apoptotic area) / (total tumor section area). **D**, Western blot analysis of MDA-MB-231 tumor homogenates ( $n = 5$  mice per group) for Akt activity [phospho-Akt (Ser<sup>473</sup>) and total Akt].  $\beta$ -Actin was used as loading control. *Columns*, densitometric measurements (by ImageJ) of phospho-Akt or total Akt bands normalized to total  $\beta$ -actin (mean  $\pm$  SE). \*,  $P < 0.05$ ; \*\*,  $P < 0.01$ .



and is frequently hyperactive in many cancer types (27), including breast cancer (28, 29), and contributes to chemotherapy resistance (30). Akt has been established as a downstream component of the PAR1-G protein-phosphatidylinositol 3-kinase axis in platelets (31, 32), and its phosphorylation in response to thrombin has been shown to occur in melanoma cells (33). Therefore, we hypothesized that P1pal-7 may regulate apoptosis by blocking the Akt survival pathway downstream of PAR1.

As predicted, treatment of MDA-MB-231 or N55 cells with thrombin caused a rapid and robust induction of Akt phosphorylation that peaked 5 min on stimulation (Fig. 3A; Supplementary Fig. S5A). Consistent with proteolytic activation of PAR1, the exogenously added SFLLRN-activating peptide also induced Akt phosphorylation but with slightly slower kinetics. PAR1-dependent Akt kinase activity was also shown by the corresponding time-dependent phosphorylation of glycogen synthase kinase 3 (34, 35) by the SFLLRN agonist peptide (Fig. 3A). Thrombin-mediated Akt phosphorylation was inhibited with P1pal-7, whereas P1pal-19EE, a negative control peptide (12, 21), was without effect (Fig. 3B; Supplementary Fig. S5B). Likewise, a small-molecule antagonist of PAR1, RWJ-56110 (36), strongly inhibited Akt phosphorylation of the MDA-MB-231 cells (Fig. 3B). Inhibition of Akt phosphorylation by P1pal-7 or RWJ-56110 resulted in corresponding decrease in Akt kinase activity as witnessed by the decrease in phospho-glycogen synthase kinase 3 (Supplementary Fig. S5C). P1pal-7 did not modulate insulin-induced or epidermal growth factor-induced Akt phosphorylation of MDA-MB-231 cells (data not shown). As anticipated, thrombin or SFLLRN was not able to induce Akt phosphorylation in the PAR1-null MCF7 and T47D carcinoma cell lines (Supplementary Fig. S5D). PAR1 knockdown by siRNA caused the MDA-MB-231 cells to lose the ability to induce glycogen synthase kinase 3 activity in response to the PAR1 agonist (Supplementary Figs. S1D and 6B). Furthermore, gene silencing of Akt1, Akt2, or Akt3 in MDA-MB-231 cells identified Akt1 as the major isoform that signals to glycogen synthase kinase 3 downstream from PAR1 (Supplementary Fig. S6A and B).

Next, we explored the significance of Akt signaling in the context of P1pal-7/Taxotere cytotoxicity. Ectopic expression of the constitutively active, myristoylated Akt in MDA-MB-231 protected against P1pal-7 cytotoxicity and eliminated its synergistic interaction with Taxotere (Fig. 3C). We then investigated the effects of Akt knockdown on apoptosis as measured by poly(ADP-ribose) polymerase (PARP) cleavage. PARP is a nuclear protein and its cleavage by caspase-3 is a reliable readout for the occurrence of apoptotic event (37). We observe here that P1pal-7 and Taxotere given together results in near-complete cleavage of PARP (Fig. 3D). Akt knockdown by siRNA confers cytotoxicity as indicated by the appearance of cleaved PARP. Notably, the addition of P1pal-7 alone does not further increase apoptosis, but the addition of Taxotere resulted in near-complete cleavage of PARP. P1pal-7 and Taxotere given together did not show significantly enhanced cytotoxicity as observed previously. To summarize, the cytotoxic effects of Akt knockdown mimicked those of P1pal-7 and rendered further addition of P1pal-7 ineffective. These results strongly suggest that P1pal-7 confers cytotoxicity by blocking the PAR1-Akt survival pathway, and Akt blockade is a critical step for the synergistic interaction of P1pal-7 and Taxotere.

**Dual therapy inhibits growth and amplifies cell death in cancer xenograft models.** We tested whether the enhanced *in vitro* cytotoxicity of the P1pal-7/Taxotere combination would be effective in estrogen-independent, aggressive breast cancer models

in nude mice. MDA-MB-231 cells were inoculated isotopically into the mammary fat pads of female nude mice and treated with vehicle (DMSO), P1pal-7, Taxotere, or P1pal-7 + Taxotere. As shown in Fig. 4A, P1pal-7 and Taxotere monotherapy did not affect tumor growth relative to vehicle. However, dual administration of P1pal-7 and Taxotere showed striking synergistic inhibition of tumor growth. These results are consistent with our cell viability data.

Next, we allowed the grafted breast carcinoma cells to form palpable tumors before initiating treatment (delayed treatment model) to test the efficacy of P1pal-7/Taxotere combination therapy against established tumors. As in the early treatment model, tumor growth rates were similar in mice given delayed P1pal-7 or Taxotere monotherapy compared with vehicle (Fig. 4A). In contrast, delayed treatment with the combination of P1pal-7 and Taxotere significantly attenuated growth rates. Visual inspection of the xenografts revealed a central area of tumor death in several of the mice treated with the combination therapy, whereas none of the mice that received monotherapy or vehicle had necrotic lesions despite the considerably larger sizes of the tumors (Supplementary Fig. S7). This observation prompted an investigation of the apoptotic state and biochemical properties of the tumors.

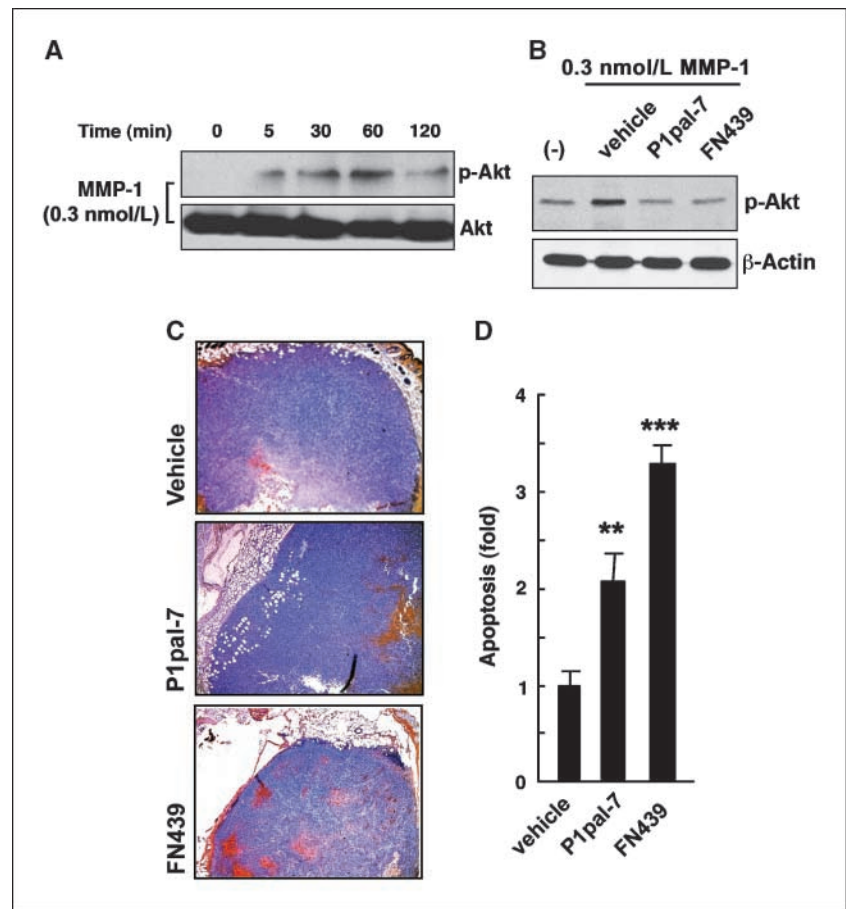
The xenograft tumors were analyzed for apoptosis using TUNEL staining. The macroscopic and magnified views of the tumor sections (Fig. 4B) showed a small central apoptotic core in the tumors of mice given either P1pal-7 or Taxotere alone or vehicle. In contrast, dual therapy resulted in massive segments of apoptosis extending well beyond the central region. The apoptotic areas were quantified and dual therapy yielded 60% apoptotic area on average, whereas monotherapy or vehicle gave 20% apoptotic area (Fig. 4C).

To investigate the acute biochemical effects of PAR1 antagonists on tumor Akt activity, we allowed MDA-MB-231 tumors ( $8 \times 10^6$  cells orthotopically injected) to grow to 200 mm<sup>3</sup> before initiating a short-term 5-day treatment of P1pal-7 (10 mg/kg) or MMP-1 inhibitor FN439 (5 mg/kg) together with a single dose of Taxotere (10 mg/kg). We found that the tumors of mice without PAR1 inhibition retained high levels of Akt phosphorylation, whereas addition of P1pal-7 or FN439 significantly attenuated Akt activity by 54% and 61%, respectively (Fig. 4D). Total Akt levels remain unchanged. These xenograft data suggest Akt as a pathophysiologic effector molecule downstream of the MMP-1/PAR1 signaling cascade in tumors.

**P1pal-7 and MMP-1 inhibitor accelerate apoptosis of breast tumors.** MMP-1 is an important mediator of cancer invasion and metastasis and has recently been identified as a novel PAR1-activating protease in cancer cells and platelets (13, 17). However, MMP-1/PAR1 signal transduction and its role in breast cancer cell survival remain unknown. Given that FN439 inhibited Akt phosphorylation in xenograft tumors (Fig. 4D), we predicted that the addition of exogenous MMP-1 to MDA-MB-231 cells would proteolytically activate PAR1 to mediate Akt phosphorylation. Indeed, we observed that 0.3 nmol/L MMP-1 triggered Akt phosphorylation with a peak signal at 1 h that subsided at 2 h (Fig. 5A). This signal is blocked by P1pal-7 and FN439, suggesting that the Akt survival pathway is indeed engaged by the MMP-1/PAR1 cascade (Fig. 5B). We also observed that MMP-1 derived from human fibroblast conditioned medium is able to activate Akt in MDA-MB-231 cells (data not shown), implicating the role of tumor stroma in PAR1-mediated tumorigenesis, invasion, and metastasis.

We have previously studied the role of MMP-1 and PAR1 in tumor growth and showed that treatment of nude mice with

**Figure 5.** MMP1-PAR1-Akt signaling cascade promotes tumor survival in mice xenograft model. **A**, MDA-MB-231 cells were starved overnight in serum-free medium and stimulated with 0.3 nmol/L MMP-1 over a period of 2 h. Cell lysates were immunoblotted with anti-phospho-Akt (Ser<sup>473</sup>). Total Akt was used as loading controls. **B**, MDA-MB-231 cells were pretreated with 3  $\mu$ mol/L P1pal-7 and 3  $\mu$ mol/L FN439 and subsequently stimulated with 0.3 nmol/L MMP-1 for 1 h. Cell lysates were immunoblotted with anti-phospho-Akt (Ser<sup>473</sup>).  $\beta$ -Actin was used as loading control. **C**, N55 cells ( $4 \times 10^6$ ) were injected into the mammary fat pads of female nude mice. After 2 d, injections with vehicle (10% DMSO), P1pal-7 (10 mg/kg), or FN439 (5 mg/kg) were initiated ( $n = 10$  mice per group). Tumors were explanted on experiment termination and sectioned for TUNEL analysis. Representative fields ( $\times 4$ ). **D**, tumor cells showing apoptosis were counted (mean  $\pm$  SE). \*\*,  $P < 0.01$ ; \*\*\*,  $P < 0.001$ .



P1pal-7 or FN439 inhibits growth of breast cancer xenografts (13). We also showed that MMP1 expression and collagenase activity were elevated in N55 tumors compared with the control mammary pads. To determine whether MMP-1 and PAR1 contribute to cell survival during tumorigenesis, we tested the effect of PAR1 blockade (P1pal-7) and MMP-1 blockade (FN439) on tumor cell death using TUNEL (Fig. 5C). There were significant 2.1- and 3.4-fold increases in the number of cells undergoing apoptosis on PAR1 or MMP-1 blockade (Fig. 5D), suggesting that the MMP-1/PAR1 cascade plays a role in protecting breast tumors from apoptotic insults.

**MMP-1/PAR1 blockade inhibits breast tumor metastasis to the lung.** The overexpression of both PAR1 and MMP-1 is strongly implicated in breast cancer invasion, metastasis, and poor overall survival (10, 38). Here, we tested the efficacy of MMP-1 and PAR1 blockade in attenuating the metastatic propensity of breast carcinoma cells using an *in vivo* model of experimental metastasis. We introduced MDA-MB-231/GFP cells via the tail vein of female nude mice and treated them with vehicle (10% DMSO), P1pal-7, or FN439. After 6 weeks, mice were sacrificed and the lungs were extracted for analysis. The lungs of mice given vehicle treatment were profusely populated with macroscopic tumor nodules at the surface (Fig. 6A). In stark contrast, tumor nodules were significantly decreased or absent on the lung surfaces of mice treated with P1pal-7 or FN439. Histologic analysis of lung sections also confirmed the efficacy of MMP-1 and PAR1 blockade against breast tumor metastasis. To ensure representative sampling of the lungs, three sections were made per lung at varying depths: the top

1/3, middle 1/3, and bottom 1/3 along the coronal plan of the lung. Counting the number of tumor nodules per lung section revealed a remarkable decrease in metastatic incidence in mice treated with P1pal-7 (75% decrease) or FN439 (88% decrease; Fig. 6B). To our knowledge, this is the first report to show inhibition of metastasis by blockade of the MMP-1/PAR1 cascade.

## Discussion

MMP-1 expression is a risk factor for overall survival of patients with invasive breast carcinoma (39). The source of MMP-1 could be stromal-derived or, in some instances, tumor-derived (16, 40). Based on recent evidence, MMP-1 is a viable therapeutic target, however, inhibitors against MMPs have not been successful. For instance, marimastat (BB-2516), a broad-spectrum MMP inhibitor, and trocade (Ro 32-3555), a MMP-1 selective inhibitor, have performed poorly in clinical trials largely due to toxicity or lack of efficacy (41). Accordingly, PAR1 may be good alternative target for the treatment of breast cancer. There is preliminary evidence from clinical trials investigating thrombosis that chronic blockade of PAR1 with a small-molecule inhibitor (SCH205831; ref. 42) is safe. It remains to be determined whether SCH205831 can effectively block MMP-1/PAR1-mediated activation of breast cancer tumors. We show, in this study, the efficacy of MMP-1/PAR1 blockade for the induction of tumor apoptosis and inhibition of metastasis to the lung.

In this report, we have examined the effects of PAR1 antagonism with a novel cell-penetrating lipopeptide, P1pal-7, on advanced-stage

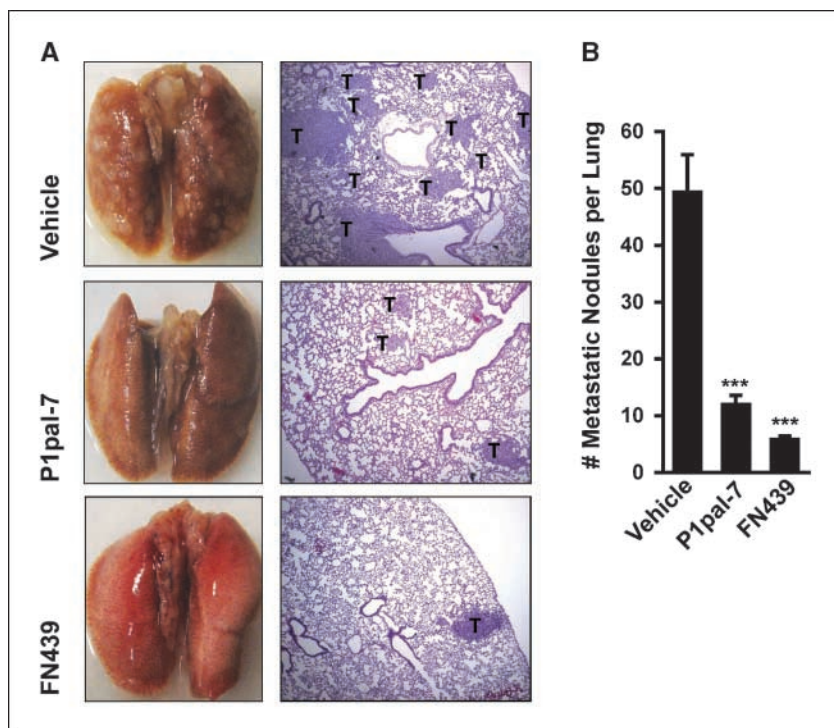


**Figure 6.** MMP-1/PAR1 blockade inhibits breast tumor metastasis to the lung. *A*, MDA-MB-231/GFP cells ( $2 \times 10^6$ ) were introduced via the tail vein of female nude mice ( $n = 5-10$  mice per group). Vehicle (10% DMSO), P1pal-7 (10 mg/kg), or FN439 (5 mg/kg) were administered 6 d/wk for 6 wk. Lungs were photographed (left column) and sectioned for H&E staining (right column; magnification,  $\times 4$ ). *T*, tumor nodule. *B*, number of metastatic tumor nodules per lung as counted under a light microscope. \*\*\*,  $P < 0.001$ .

breast cancer cells both *in vitro* and in animals. The data presented here suggest that PAR1 blockade by P1pal-7 may be a viable approach to affect PAR1-mediated survival pathways and may synergistically enhance cytotoxicity and apoptosis with antitumor agents, as exemplified by Taxotere, in models of breast cancer. Combination treatment of breast tumors with P1pal-7 and Taxotere significantly inhibited tumor growth and caused massive apoptosis. Our present study characterizes the involvement of the prominent cell survival mediator, Akt, in the context of PAR1 blockade and combination therapy. While investigating the role of PAR1 in growth and survival, we observed that breast cancer cells expressing PAR1 have increased proliferative potential but are simultaneously vulnerable to PAR1 blockade. In fact, stable expression of PAR1 (MCF7-PAR1/N55) is sufficient in rendering P1pal-7 sensitivity to the MCF7 cell line. PAR1 blockade also had cytotoxic effects against MDA-MB-231 and Bt549 breast cancer cell lines naturally expressing high levels of PAR1, representing an advanced, endocrine therapy-resistant form of breast cancer (43, 44). PAR1, hence, provides a novel mode of

attack against advanced breast cancer models with aggressive phenotypes.

### Disclosure of Potential Conflicts of Interest

Tufts Medical Center has out-licensed the peptidic, P1pal-7, used in this article. L. Covic and A. Kuliopulos: Consultant/advisory board, Ascent Therapeutics. The other authors disclosed no potential conflicts of interest.

### Acknowledgments

Received 1/17/09; revised 5/6/09; accepted 5/26/09; published OnlineFirst 7/21/09.

**Grant support:** NIH grants CA104406 (L. Covic) and CA122992, HL64701, and HL57905 (A. Kuliopulos); Susan G. Komen grants BCTR0706763 (L. Covic) and BCTR0601348 (A. Kuliopulos); and Aid for Cancer Research fellowship (E. Yang).

The costs of publication of this article were defrayed in part by the payment of page charges. This article must therefore be hereby marked *advertisement* in accordance with 18 U.S.C. Section 1734 solely to indicate this fact.

We thank Vishal Trivedi, Akiko Hata, and Larry Feig for insightful discussions and invaluable advice; Katherine Lazarides for assistance with the xenograft experiments; Gary Sahagian and Kai Tao for the use of Xenogen IVIS 200 Biophotonic Imager; Charlotte Kuperwasser for the use of her microscope and camera; and Andrew Leger, Leila Sevigny, George Koukos, Shaida Andrabi, Maria Chatziapostolou, Cristina Gavrilescu, Theresa DiMeo, Vandana Iyer, and Patricia Keller for expert advice.

### References

- Jemal A, Siegel R, Ward E, Murray T, Xu J, Thun MJ. Cancer statistics, 2007. *CA Cancer J Clin* 2007;57:43-66.
- Greenberg PA, Hortobagyi GN, Smith TL, Ziegler LD, Frye DK, Buzdar AU. Long-term follow-up of patients with complete remission following combination chemotherapy for metastatic breast cancer. *J Clin Oncol* 1996;14:2197-205.
- Orlando L, Colleoni M, Fedele P, et al. Management of advanced breast cancer. *Ann Oncol* 2007;18 Suppl 6: vi74-6.
- Ihemelandu CU, Leffall LD, Jr., Dewitty RL, et al. Molecular breast cancer subtypes in premenopausal and postmenopausal African-American women: age-specific prevalence and survival. *J Surg Res* 2007;143:109-18.
- Dalerba P, Cho RW, Clarke MF. Cancer stem cells: models and concepts. *Annu Rev Med* 2007;58:267-84.
- Granovsky-Grisaru S, Zaidoun S, Grisaru D, et al. The pattern of protease activated receptor 1 (PAR1) expression in endometrial carcinoma. *Gynecol Oncol* 2006;103:802-6.
- Grisaru-Granovsky S, Salah Z, Mao M, Pruss D, Beller U, Bar-Shavit R. Differential expression of protease activated receptor 1 (Par1) and pY397FAK in benign and malignant human ovarian tissue samples. *Int J Cancer* 2005;113:372-8.
- Heider I, Schulze B, Oswald E, Henklein P, Scheele J, Kaufmann R. PAR1-type thrombin receptor stimulates migration and matrix adhesion of human colon carcinoma cells by a PKC $\epsilon$ -dependent mechanism. *Oncol Res* 2004;14:475-82.
- Greenberg DL, Mize GJ, Takayama TK. Protease-activated receptor mediated RhoA signaling and cytoskeletal reorganization in LNCaP cells. *Biochemistry* 2003;42:702-9.

10. Even-Ram S, Uziely B, Cohen P, et al. Thrombin receptor overexpression in malignant and physiological invasion processes. *Nat Med* 1998;4:909-14.
11. Nierodzki ML, Kajumo F, Karparkin S. Effect of thrombin treatment of tumor cells on adhesion of tumor cells to platelets *in vitro* and tumor metastasis *in vivo*. *Cancer Res* 1992;52:3267-72.
12. Agarwal A, Covic L, Sevigny LM, et al. Targeting a metalloprotease-PAR1 signaling system with cell-penetrating pепducins inhibits angiogenesis, ascites, and progression of ovarian cancer. *Mol Cancer Ther* 2008;7:2746-57.
13. Boire A, Covic L, Agarwal A, Jacques S, Sherif S, Kuliopulos A. PAR1 is a matrix metalloprotease-1 receptor that promotes invasion and tumorigenesis of breast cancer cells. *Cell* 2005;120:303-13.
14. Kuliopulos A, Covic L, Seeley SK, Sheridan PJ, Helin J, Costello CE. Plasmin desensitization of the PAR1 thrombin receptor: kinetics, sites of truncation, and implications for thrombolytic therapy. *Biochemistry* 1999;38:4572-85.
15. Ossovskaya VS, Bunnett NW. Protease-activated receptors: contribution to physiology and disease. *Physiol Rev* 2004;84:579-621.
16. Goerge T, Barg A, Schnaeker EM, et al. Tumor-derived matrix metalloproteinase-1 targets endothelial proteinase-activated receptor 1 promoting endothelial cell activation. *Cancer Res* 2006;66:7766-74.
17. Trivedi V, Boire A, Tchernychev B, et al. Platelet matrix metalloprotease-1 mediates thrombogenesis by activating PAR1 at a cryptic ligand site. *Cell* 2009;137:332-43.
18. Murray GI, Duncan ME, O'Neil P, McKay JA, Melvin WT, Fothergill JE. Matrix metalloproteinase-1 is associated with poor prognosis in oesophageal cancer. *J Pathol* 1998;185:256-61.
19. Murray GI, Duncan ME, O'Neil P, Melvin WT, Fothergill JE. Matrix metalloproteinase-1 is associated with poor prognosis in colorectal cancer. *Nat Med* 1996;2:461-2.
20. Poola I, DeWitty RL, Marshalleck JJ, Bhatnagar R, Abraham J, Leffall LD. Identification of MMP-1 as a putative breast cancer predictive marker by global gene expression analysis. *Nat Med* 2005;11:481-3.
21. Covic L, Gresser AL, Talavera J, Swift S, Kuliopulos A. Activation and inhibition of G protein-coupled receptors by cell-penetrating membrane-tethered peptides. *Proc Natl Acad Sci U S A* 2002;99:643-8.
22. Ramaswamy S, Nakamura N, Vazquez F, et al. Regulation of G<sub>1</sub> progression by the PTEN tumor suppressor protein is linked to inhibition of the phosphatidylinositol 3-kinase/Akt pathway. *Proc Natl Acad Sci U S A* 1999;96:2110-5.
23. Kamath L, Meydani A, Foss F, Kuliopulos A. Signaling from protease-activated receptor-1 inhibits migration and invasion of breast cancer cells. *Cancer Res* 2001;61:5933-40.
24. Nguyen N, Kuliopulos A, Graham RA, Covic L. Tumor-derived Cyr61(CCN1) promotes stromal matrix metalloproteinase-1 production and protease-activated receptor 1-dependent migration of breast cancer cells. *Cancer Res* 2006;66:2658-65.
25. Chou TC, Talalay P. Quantitative analysis of dose-effect relationships: the combined effects of multiple drugs or enzyme inhibitors. *Adv Enzyme Regul* 1984;22:27-55.
26. Altomare DA, Testa JR. Perturbations of the AKT signaling pathway in human cancer. *Oncogene* 2005;24:7455-64.
27. Bellacosa A, Kumar CC, Di Cristofano A, Testa JR. Activation of AKT kinases in cancer: implications for therapeutic targeting. *Adv Cancer Res* 2005;94:29-86.
28. Carpten JD, Faber AL, Horn C, et al. A transforming mutation in the pleckstrin homology domain of AKT1 in cancer. *Nature* 2007;448:439-44.
29. Lin HJ, Hsieh FC, Song H, Lin J. Elevated phosphorylation and activation of PDK-1/AKT pathway in human breast cancer. *Br J Cancer* 2005;93:1372-81.
30. Knuefermann C, Lu Y, Liu B, et al. HER2/PI-3K/Akt activation leads to a multidrug resistance in human breast adenocarcinoma cells. *Oncogene* 2003;22:3205-12.
31. Resendiz JC, Kroll MH, Lassila R. Protease activated receptors-induced Akt activation—regulation and possible function. *J Thromb Haemost* 2007;5:2484-93.
32. Kim S, Jin J, Kunapuli SP. Akt activation in platelets depends on G<sub>i</sub> signaling pathways. *J Biol Chem* 2004;279:4186-95.
33. Salah Z, Maoz M, Pokroy E, Lotem M, Bar-Shavit R, Uziely B. Protease-activated receptor-1 (hPar1), a survival factor eliciting tumor progression. *Mol Cancer Res* 2007;5:229-40.
34. Cross DA, Alessi DR, Cohen P, Andjelkovich M, Hemmings BA. Inhibition of glycogen synthase kinase-3 by insulin mediated by protein kinase B. *Nature* 1995;378:785-9.
35. Srivastava AK, Pandey SK. Potential mechanism(s) involved in the regulation of glycogen synthesis by insulin. *Mol Cell Biochem* 1998;182:135-41.
36. Andrade-Gordon P, Maryanoff BE, Derian CK, et al. Design, synthesis, and biological characterization of a peptide-mimetic antagonist for a tethered-ligand receptor. *Proc Natl Acad Sci U S A* 1999;96:12257-62.
37. He J, Whitacre CM, Xue LY, Berger NA, Oleinick NL. Protease activation and cleavage of poly(ADP-ribose) polymerase: an integral part of apoptosis in response to photodynamic treatment. *Cancer Res* 1998;58:940-6.
38. McGowan PM, Duffy MJ. Matrix metalloproteinase expression and outcome in patients with breast cancer: analysis of a published database. *Ann Oncol* 2008;19:1566-72.
39. Cheng S, Tada M, Hida Y, et al. High MMP-1 mRNA expression is a risk factor for disease-free and overall survivals in patients with invasive breast carcinoma. *J Surg Res* 2008;146:104-9.
40. Blackburn JS, Brinckerhoff CE. Matrix metalloproteinase-1 and thrombin differentially activate gene expression in endothelial cells via PAR-1 and promote angiogenesis. *Am J Pathol* 2008;173:1736-46.
41. Sparano JA, Bernardo P, Stephenson P, et al. Randomized phase III trial of marimastat versus placebo in patients with metastatic breast cancer who have responding or stable disease after first-line chemotherapy: Eastern Cooperative Oncology Group trial E2196. *J Clin Oncol* 2004;22:4683-90.
42. Chackalamannil S, Xia Y, Greenlee WJ, et al. Discovery of potent orally active thrombin receptor (protease activated receptor 1) antagonists as novel antithrombotic agents. *J Med Chem* 2005;48:5884-7.
43. Thompson EW, Paik S, Brunner N, et al. Association of increased basement membrane invasiveness with absence of estrogen receptor and expression of vimentin in human breast cancer cell lines. *J Cell Physiol* 1992;150:534-44.
44. Osborne CK, Hobbs K, Clark GM. Effect of estrogens and antiestrogens on growth of human breast cancer cells in athymic nude mice. *Cancer Res* 1985;45:584-90.

# Cancer Research

The Journal of Cancer Research (1916–1930) | The American Journal of Cancer (1931–1940)

## Blockade of PAR1 Signaling with Cell-Penetrating Pepducins Inhibits Akt Survival Pathways in Breast Cancer Cells and Suppresses Tumor Survival and Metastasis

Eric Yang, Adrienne Boire, Anika Agarwal, et al.

*Cancer Res* 2009;69:6223-6231. Published OnlineFirst July 21, 2009.

### Updated version

Access the most recent version of this article at:  
doi:[10.1158/0008-5472.CAN-09-0187](https://doi.org/10.1158/0008-5472.CAN-09-0187)

### Supplementary Material

Access the most recent supplemental material at:  
<http://cancerres.aacrjournals.org/content/suppl/2009/07/17/0008-5472.CAN-09-0187.DC1>

### Cited articles

This article cites 43 articles, 14 of which you can access for free at:  
<http://cancerres.aacrjournals.org/content/69/15/6223.full#ref-list-1>

### Citing articles

This article has been cited by 19 HighWire-hosted articles. Access the articles at:  
<http://cancerres.aacrjournals.org/content/69/15/6223.full#related-urls>

### E-mail alerts

[Sign up to receive free email-alerts](#) related to this article or journal.

### Reprints and Subscriptions

To order reprints of this article or to subscribe to the journal, contact the AACR Publications Department at [pubs@aacr.org](mailto:pubs@aacr.org).

### Permissions

To request permission to re-use all or part of this article, use this link  
<http://cancerres.aacrjournals.org/content/69/15/6223>.  
Click on "Request Permissions" which will take you to the Copyright Clearance Center's (CCC) Rightslink site.